Cell, Vol. 57, 645–658, May 19, 1989, Copyright © 1989 by Cell Press

The Homeotic Gene *fork head* Encodes a Nuclear Protein and Is Expressed in the Terminal Regions of the Drosophila Embryo

Detlef Weigel,* Gerd Jürgens,† Frank Küttner,* Eveline Seifert,* and Herbert Jäckle*
Max-Planck-Institut für Entwicklungsbiologie
Spemannstrasse 35/II
D-7400 Tübingen
Federal Republic of Germany

Summary

The region-specific homeotic gene *fork head (fkh)* promotes terminal as opposed to segmental development in the Drosophila embryo. We have cloned the *fkh* region by chromosomal walking. P element–mediated germ-line transformation and sequence comparison of wild-type and mutant alleles identify the *fkh* gene within the cloned region. *fkh* is expressed in the early embryo in the two terminal domains that are homeotically transformed in *fkh* mutant embryos. The nuclear localization of the *fkh* protein suggests that *fkh* regulates the transcription of other, subordinate, genes. The *fkh* gene product, however, does not contain a known protein motif, such as the homeodomain or the zinc fingers, nor is it similar in sequence to any other known protein.

Introduction

Segment diversification in insects is brought about by the action of homeotic genes during development. Although homeotic genes in the fruit fly Drosophila melanogaster have been the focus of many genetic and molecular studies, attention has been paid almost exclusively to the development of the overtly segmented, central region in the embryo (reviewed by Akam, 1987; Ingham, 1988).

The homeotic selector genes of the Antennapedia (ANT-C) and bithorax (BX-C) complexes that direct parasegment-specific pathways (Martinez-Arias and Lawrence, 1985) in the central region of the Drosophila embryo, i.e. parasegments (PS) 0–15 (see Akam, 1987; Ingham, 1988), share certain features at both the genetic and the molecular level. Specifically, all selector genes encode homeodomain-containing proteins (Gehring and Hiromi, 1986) that can bind to specific DNA sequences and thus are able to regulate transcription of other genes (Desplan et al., 1985, 1988; Hoey and Levine, 1988).

Recently, a novel class of homeotic genes has been discovered. Because these genes act independently of the homeotic selector gene network and are not regulated by the *Polycomb* group genes that control expression of homeotic selector genes, the term "region-specific homeotic genes" was proposed (Jürgens, 1988; Jürgens and Weigel, 1988). The prototype gene of this class is *spalt (sal)*, which is active in both posterior head (PS 1 and 2) and anterior tail (PS 14 and 15). The genetic differences to the homeotic selector genes are paralleled by the completely different molecular structure of the *sal* gene, which encodes a small protein without a homeodomain (Frei et al., 1988).

Like *sal*, the *fork head (fkh)* gene is required in separate domains at the ends of the Drosophila embryo. The *fkh* domains are located more anteriorly in the head and more posteriorly in the tail than the *sal* domains. In both domains, *fkh* mutations cause homeotic transformation of the ectodermal portions of the gut: foregut and hindgut are replaced by ectopic head structures in *fkh* mutant embryos. Foregut and hindgut lie outside the segmented body region of PS 0–15 in which the homeotic selector genes and the *sal* gene act. They develop from the stomodaeum and the proctodaeum, which constitute the terminal regions of the ectodermal anlage in the blastoderm embryo (Hartenstein et al., 1985). Since the ectopic head structures in *fkh* mutant embryos develop independently of the activity of ANT-C and BX-C genes, it appears reasonable to conclude that the *fkh* gene promotes terminal development directly from a parasegmental ground state. This ground state corresponds to the pattern of any body parasegment in the absence of the ANT-C and BX-C genes (Jürgens and Weigel, 1988). The anlagen of foregut and hindgut had not been recognized before as being homologous to the parasegmental anlagen of the overtly segmented body region. The interpretation of the *fkh* domains as cryptic segment primordia is supported by the repetitive expression patterns of some segmentation genes that extend into these terminal regions (Baumgartner et al., 1987; Baker, 1988). One of these genes is the segment polarity gene *wingless*, which is expressed in 21 stripes throughout the embryo, with the first stripe corresponding to the foregut primordium and the last one to the hindgut primordium (Baker, 1988).

Here, we report the molecular identification of the *fkh* gene, its structure, and its expression pattern. Consistent with the mutant phenotype, *fkh* is expressed in two terminal domains of the early embryo. The *fkh* protein does not contain a homeodomain, nor is it similar to the *sal* protein or any other known protein. However, the *fkh* protein is localized in the nucleus and therefore could act as a transcriptional regulator.

Results

Cloning of the *fkh* Region and Identification of Embryonic Transcripts

The *fkh* gene maps cytologically to polytene chromosome bands 98D2,3 (Jürgens and Weigel, 1988). The cDNA clone E7Δ6, which had been isolated by virtue of cross-hybridization to EGF-like sequences (Knust et al., 1987), was used to initiate a chromosomal walk in the region of

* Present address: Universität München, Institut für Genetik und Mikrobiologie, Maria-Ward-Strasse 1a, D-8000 München 19, Federal Republic of Germany
† Present address: Universität Tübingen, Institut für Biologie II (Genetik), Auf der Morgenstelle 28, D-7400 Tübingen, Federal Republic of Germany

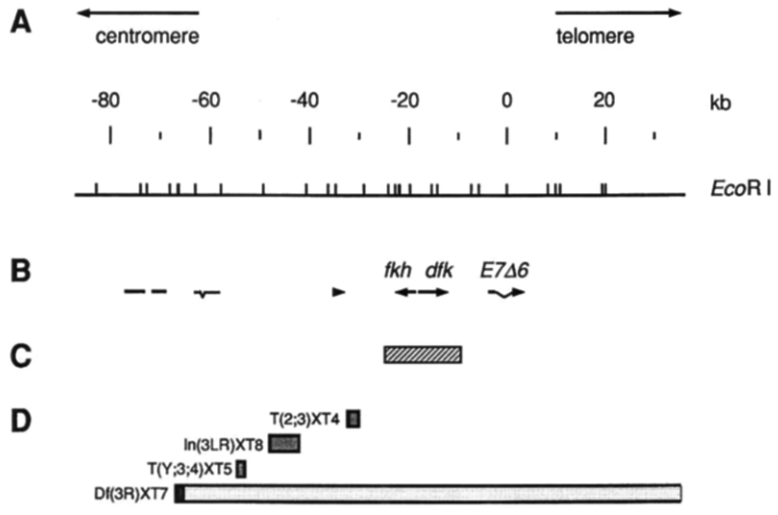

Figure 1. Molecular Organization of the *fkh* Region

(A) Chromosomal orientation and EcoRI sites of cloned genomic DNA. The cytological extent of the walk was determined by in situ hybridization to polytene chromosomes of wild-type larvae. Zero on the scale corresponds to the EcoRI site spanned by the E7Δ6 cDNA clone.
(B) Embryonic transcripts. Orientation of four transcripts was determined by hybridization of single-stranded RNA probes to Northern blots. E7Δ6 corresponds to the cDNA clone with which the chromosomal walk was initiated. *fkh*, *fork head*. *dfk*, *distal of fork head*.
(C) Extent of the 15.3 kb NotI–SpeI fragment used for germ-line transformation. It covers about 8.8 kb of *fkh* upstream and about 2.5 kb of downstream sequences.
(D) Breakpoints of *fkh* alleles as determined by genomic Southern blots, in situ hybridization to polytene chromosomes of mutant larvae, and cloning of mutant DNA. The darkly shaded bars indicate the smallest wild-type fragment to which the breakpoints were mapped. The lightly shaded bar indicates the extent of deleted DNA in *Df(3R)XT7*.

interest. We isolated about 120 kb of genomic DNA covering the chromosomal interval 98D1 to 98E1 (Figure 1). Three out of eight *fkh* alleles are associated with cytologically visible chromosome rearrangements (Jürgens and Weigel, 1988). Their breakpoints are scattered over about 25 kb within the cloned region. In addition, a fourth allele is deficient for most of the cloned DNA (Figure 1).

Since all three breakpoint-associated alleles produce weak *fkh* phenotypes (Jürgens and Weigel, 1988), they were presumed not to disrupt the *fkh* transcription unit itself but rather to remove only *cis*-regulatory elements. Furthermore, the translocation fkh^{XT4} segregates a terminal deficiency that uncovers the *fkh* locus (D. Weigel, unpublished data). Therefore, the *fkh* gene should lie distal to the fkh^{XT4} breakpoint. "Reverse" and conventional Northern blot analyses and cloning of cDNAs identified at least seven embryonic transcripts in the cloned region (Figure 1). The temporal expression patterns of two of these transcripts immediately distal to the fkh^{XT4} breakpoint meet the requirements of *fkh* gene activity as determined by genetic and embryological experiments (Figure 2). Specifically, transcripts are virtually absent from maternal RNA, which is consistent with the observation that lack of *fkh* gene activity in the female germ line does not affect the expression of the *fkh* mutant phenotype (Jürgens and Weigel, 1988). Transcripts start to accumulate at 2–4 hr of

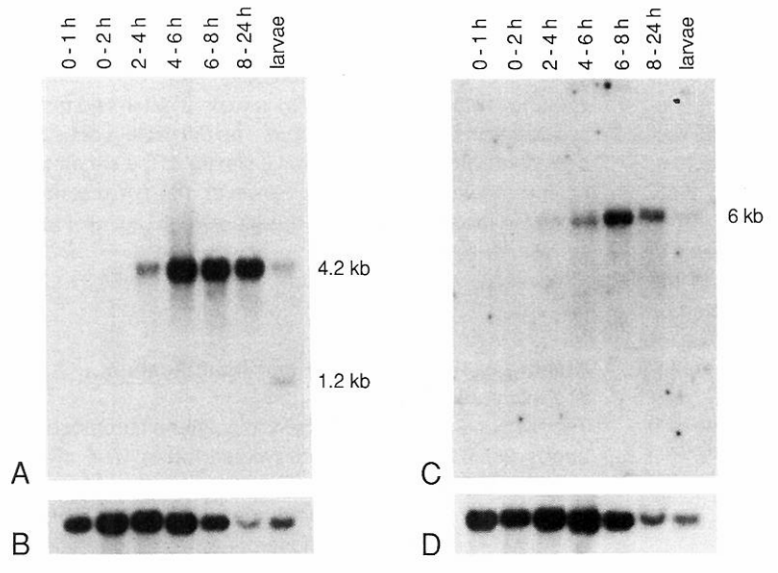

Figure 2. Northern Blot Analyses of *fkh* (A) and *dfk* (C)

In (A), the same probe as for in situ hybridization to tissue sections was used (see Experimental Procedures). Note that in larvae a second, smaller transcript is detected by the *fkh* probe. Interestingly, the larva-specific *fkh* transcript of 1.2 kb is shorter than the 1.5 kb open reading frame used in the large 4.2 kb transcript (see Figures 5, and 6). In (C), a 2.3 kb long cDNA clone, cF13 (see Figure 5), was used. Five micrograms of poly(A)-enriched RNA extracted from embryos of different age (times in hours at 25°C) and from larvae of predominantly third instar was loaded. To estimate the amount of poly(A)$^+$ RNA, the blots were reprobed with a tubulin clone (B, D; kindly provided by R. Renkawitz-Pohl, Munich). Sizes of the detected RNAs were compared with an RNA standard (BRL).

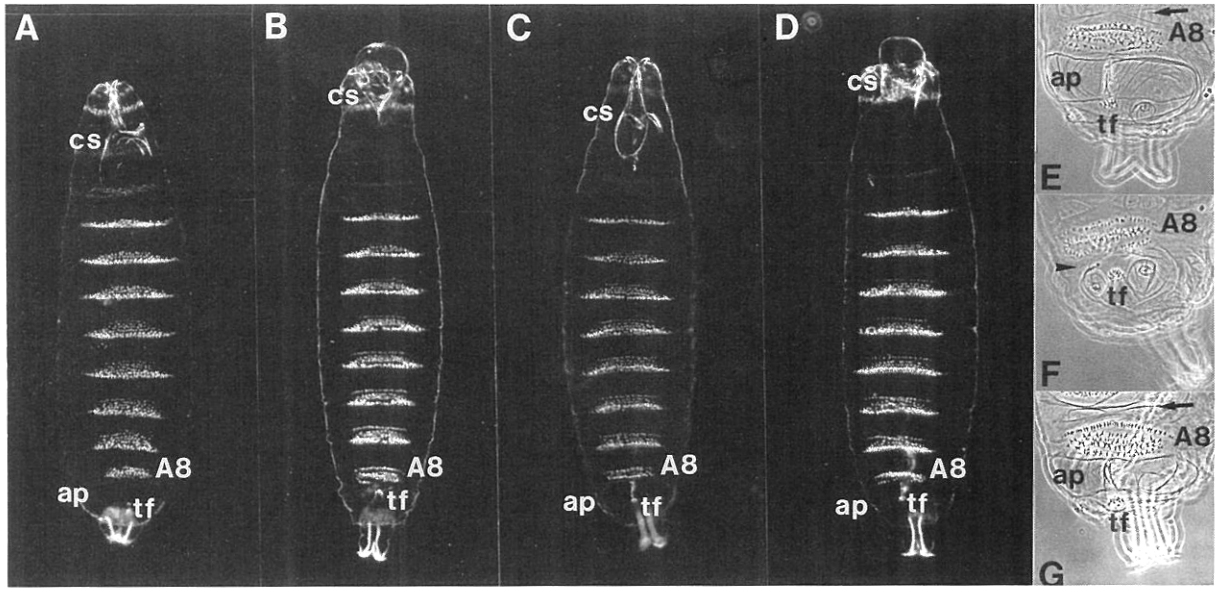

Figure 3. Phenotypic Rescue of an Amorphic *fkh* Allele by P Element–Mediated Germ-Line Transformation

Comparison of cuticle preparations of wild-type (A, E), amorphic fkh^3 (B, F), hypomorphic fkh^3/fkh^{XT5} (C) and intermediate *P[NS-fkh2]*; fkh^3 (D, G) larvae. As in the amorphic mutant larva (B), head involution has failed in the transformed larva (D). Head involution is not perturbed in the hypomorphic condition (C). In contrast to the amorphic phenotype (F), the tail of the transformed larva (G) is almost normal. The anal pads (ap) and the hindgut (out of focus; arrow in E, G), that are missing in the amorph (arrowhead in F), are present in the transformed larva (G). (A8) ventral denticle band of eighth abdominal segment. (cs) cephalopharyngeal skeleton. (tf) anal tuft. (A)–(D). Dark-field. (E)–(G). Phase-contrast.

embryonic development, i.e. around the blastoderm stage when determination of the ectodermal anlagen occurs (see Akam, 1987; Technau, 1987).

Identification of the *fkh* Gene

To identify DNA fragments encoding essential *fkh* wild-type functions, we employed P element–mediated germ-line transformation. A 15.3 kb NotI–SpeI fragment, (Figure 1) that probably encompasses the complete genomic DNA coding for the two *fkh* candidate transcripts was cloned into the P element vector pW8 (see Experimental Procedures), and the resulting construct was used to transform the germ line of *fkh* mutant flies. Examination of the cuticle pattern of transformed embryos revealed that the 15.3 kb fragment partially suppressed the phenotype of an amorphic *fkh* allele. The phenotype of amorphic fkh^3 embryos carrying the recombinant transposon P[NS-*fkh*] is intermediate between the strong phenotype of amorphic and the weak phenotype of hypomorphic *fkh* alleles (Figure 3; see Jürgens and Weigel, 1988). Specifically, the posterior end develops almost normally, whereas the anterior end still exhibits the strong phenotype typical of amorphic alleles. Thus, the 15.3 kb fragment includes essential *fkh* sequences, but it does not contain all regulatory elements of the *fkh* gene. This is in agreement with the finding that all weak *fkh* alleles leave more contiguous DNA sequences intact than are contained within the 15.3 kb fragment (see Figure 1).

On the basis of the P element–mediated transformation, we were unable to decide which of the two transcripts included in the 15.3 kb genomic fragment was the *fkh* transcript. Four amorphic *fkh* alleles appeared to be point mutants, because we could not detect any abnormality by genomic Southern blot analysis. Since the spatial expression pattern suggested that the proximal transcript was most likely to be the *fkh* transcript (see below), we determined the wild-type sequence of this transcript and compared it with the sequence of the four apparent point mutants. A restriction fragment length polymorphism allowed for cloning of mutant DNA from flies heterozygous for each of the four alleles (see Experimental Procedures). In all four alleles, a region that corresponds to the first two-thirds of the large open reading frame in the wild-type transcript was sequenced. In each allele, a single deviation from the wild-type sequence was found (Figure 4). The X-ray-induced allele fkh^{XT6} carries an 11 bp deletion leading to a frame shift after 7 amino acids of the wild-type protein. The two EMS-induced alleles fkh^1 and fkh^3 exhibit single base pair transitions that create premature stop codons at residues 254 and 63, respectively. The 17 bp deletion in the EMS-induced allele fkh^2 is accompanied by a 2 bp insertion, so that the open reading frame of the wild-type is retained. The deduced mutant protein lacks six amino acids, which are now replaced by a different one. Since fkh^2—like the other three alleles—is an amorphic allele, this deletion appears to affect an essential domain of the *fkh* protein. The sequence changes in all four alleles unambiguously identify the *fkh* transcript within the fragment used for germ-line transformation.

DNA Sequence of the *fkh* Gene and Properties of the *fkh* Protein

The sequence of 5.7 kb of genomic wild-type DNA and of three different embryonic *fkh* cDNAs was determined

aa	6							13
wild-type	GCG	GAG	CCG	CCT	CCG	AGC	AGT	GCT
	Ala	Glu	Pro	Pro	Ser	Ser	Ser	Ala
fkh^{xr6}	GCG	GAG	...	...	...	..CAG		TGC
	Ala	Glu	...	...	...	..*Gln*		*Cys*
aa	56							63
wild-type	GGC	AGC	ATG	AGT	CCC	CTG	GCT	CGA
	Gly	Ser	Met	Ser	Pro	Leu	Ala	Arg
fkh^{3}	GGC	AGC	ATG	AGT	CCC	CTG	GCT	*TGA*
	Gly	Ser	Met	Ser	Pro	Leu	Ala	***
aa	231							238
wild-type	TTG	ACG	CTC	TCG	GAG	ATC	TAT	CAG
	Leu	Thr	Leu	Ser	Glu	Ile	Tyr	Gln
fkh^{2}	TTG	*ATC*	...	...	...	...	...	CAG
	Leu	*Ile*	...	...	...	...	...	Gln
aa	247							254
wild-type	TAC	AGG	CAG	AAT	CAG	CAG	CGC	TGG
	Tyr	Arg	Gln	Asn	Gln	Gln	Arg	Trp
fkh^{1}	TAC	AGG	CAG	AAT	CAG	CAG	CGC	TGA
	Tyr	Arg	Gln	Asn	Gln	Gln	Arg	***

Figure 4. Sequence Changes in Four *fkh* Alleles

Nucleotide and deduced amino acid sequence of wild-type and mutants are compared. Deletions are marked by (. . .), bases and amino acids deviating from the wild-type sequence are printed in italic, (***) indicates stopcodons. The numbers refer to codons and amino acids of the wild-type sequence.

(Figure 5). The combined lengths of the sequenced cDNAs add up to 4,004 bp. Compared with the size of the embryonic poly(A)$^+$ *fkh* transcript of about 4.2 kb, the sequenced cDNAs are probably close to full length. The cDNA sequence confirms the direction of transcription, which implies that the breakpoints of all weak *fkh* alleles lie downstream of the *fkh* transcript. The intronless transcript contains a single large open reading frame of 1,530 bp starting with an ATG preceded by the sequence CATC in good agreement with the Drosophila translation start consensus sequence ^{C}/AAA^{A}/cATG (Figure 6; see Cavener, 1987). Three other ATGs in the 5′ untranslated leader are all followed immediately by stop codons. The usage of the large open reading frame is confirmed by the appearance of stop codons disrupting this frame in two of the mutant alleles (see above). The protein predicted by the large open reading frame is 510 amino acids long and has a calculated molecular weight of 54.3 kd. Computer searches did not reveal any significant sequence similarity to known proteins. Particularly, the protein does not contain a homeodomain characteristic of the homeotic selector genes of the ANT-C and BX-C (Gehring and Hiromi, 1986), nor does it exhibit sequence similarity to the region-specific homeotic gene *sal* (Frei et al., 1988).

To determine the subcellular localization of the protein, we raised polyclonal antibodies directed against a bacterial *lacZ–fkh* fusion protein (see Experimental Procedures) and visualized *fkh* protein in Drosophila embryos by antibody staining. The *fkh* protein is restricted to nuclei, as can be observed clearly in sections of antibody-stained embryos (Figure 7). Thus, the *fkh* gene encodes a nuclear protein of novel structure.

The sequence of two cDNA clones derived from the transcription unit called *distal of fork head (dfk)*, which is adjacent to the *fkh* gene, was partially determined. Sequence analysis confirmed that the *dfk* gene is transcribed in opposite direction to the *fkh* gene. The 5′ end of the longest *dfk* cDNA is less than 500 bp from the 5′ end of the longest *fkh* cDNA on the genomic map. Although we did not determine the transcription start sites of the two genes exactly, we conclude that their transcription starts are less than 500 bp apart.

Expression of the *fkh* Gene in Two Terminal Domains of the Blastoderm Embryo

Phenotypic analysis had shown that *fkh* gene activity is required in two terminal domains of the embryo where its absence causes homeotic transformations (Jürgens and Weigel, 1988). If *fkh* acts as a developmental switch gene, it should already be expressed in its terminal domains at early stages.

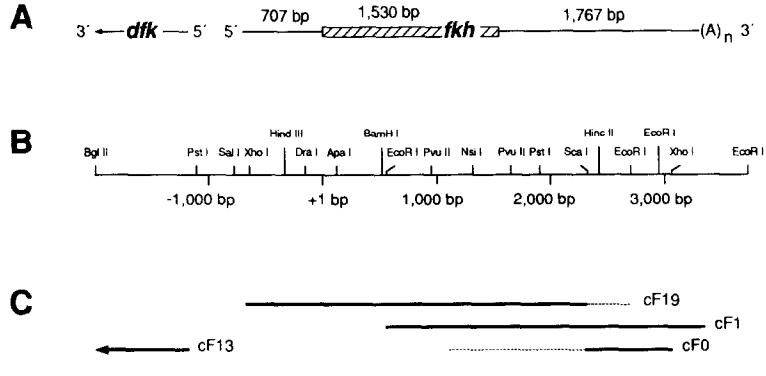

Figure 5. Transcript Structure of the *fkh* Region

(A) Transcript structure as deduced from comparison of genomic and cDNA sequence. The 1,530 bp open reading frame of *fkh* is indicated by a bar. The 5′ untranslated leader is at least 707 bp long; the 3′ untranslated trailer is 1,767 bp long.

(B) Restriction sites of the sequenced genomic fragment from a BglII to an EcoRI site. +1 bp denotes the translation start.

(C) Sequenced portions of cDNAs are indicated by solid bars; unsequenced portions by dashed lines. The *fkh* cDNA cF0 appears to have lost its authentic 3′ end, since it misses a poly(A) tail. The *dfk* cDNA cF13 is 2.3 kb long. In addition to the 5′ end, the 3′ end of cF13 was sequenced, where an $(A)_{13}$ stretch that is also present in the genomic DNA was found. This cDNA is obviously the result of internal priming, as are all other isolated *dfk* cDNAs, since all analyzed *dfk* cDNA clones represent only sequences homologous to the 5′ portion of the 6 kb *dfk* transcript (data not shown).

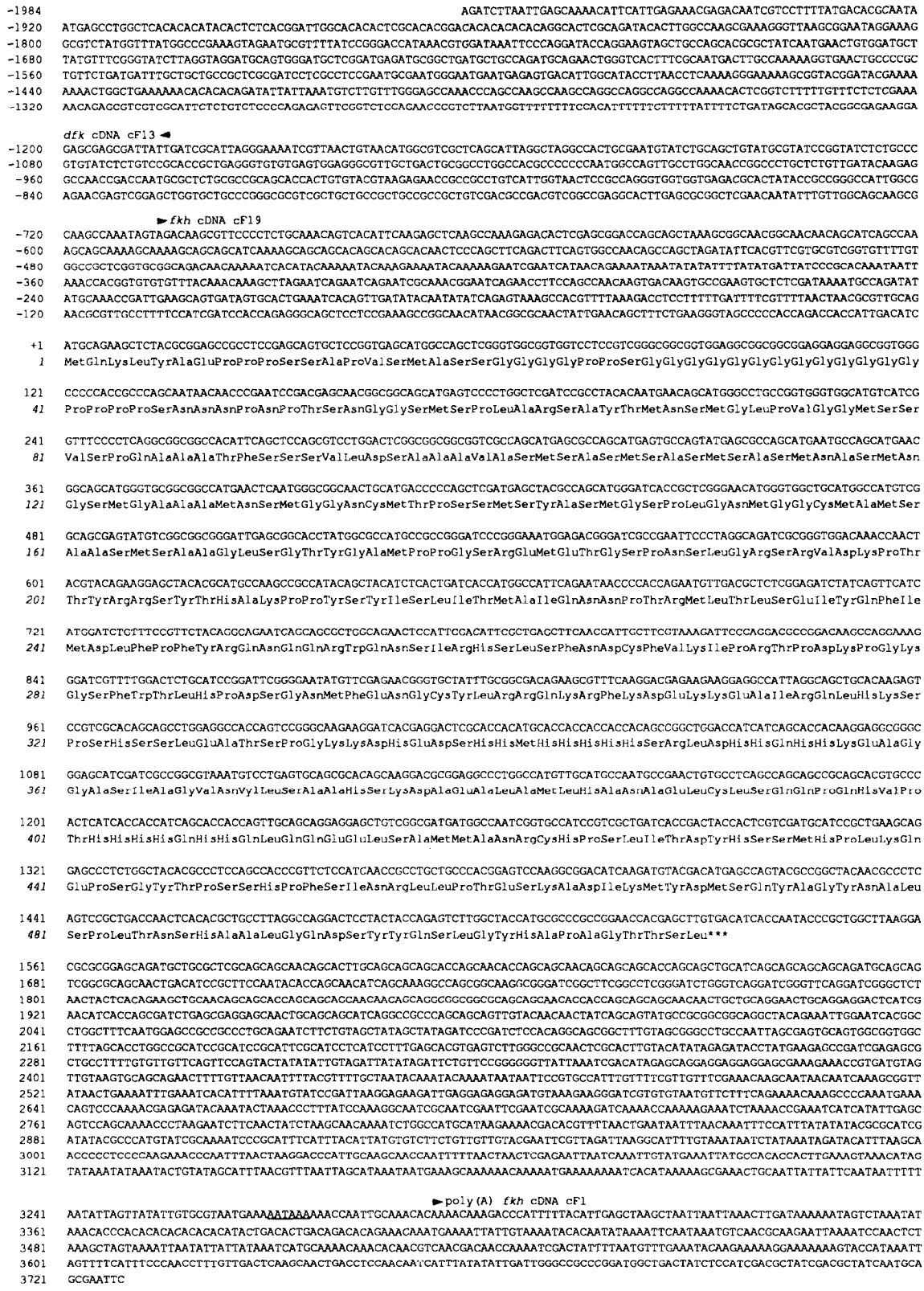

Figure 6. Nucleotide Sequence of the *fkh* Gene

The completely sequenced genomic fragment is 5,712 bp long. +1 bp denotes the start of the *fkh* open reading frame. The deduced amino acids are numbered in italics. The 5′ ends of the longest *fkh* and *dfk* cDNAs are indicated by arrowheads, as is the poly(A) tail at the 3′ end of another *fkh* cDNA. The polyadenylation signal AATAAA is underlined. cDNA and genomic sequence are identical with one exception. The hexamere GCAATC in the 3′ noncoding trailer of the *fkh* transcript immediately preceding the EcoRI site at +2698 bp is present in the cDNAs in three instead of two copies as in the genomic DNA. It probably represents a cryptic simple sequence that changes rapidly during evolution (see Tautz et al., 1986).

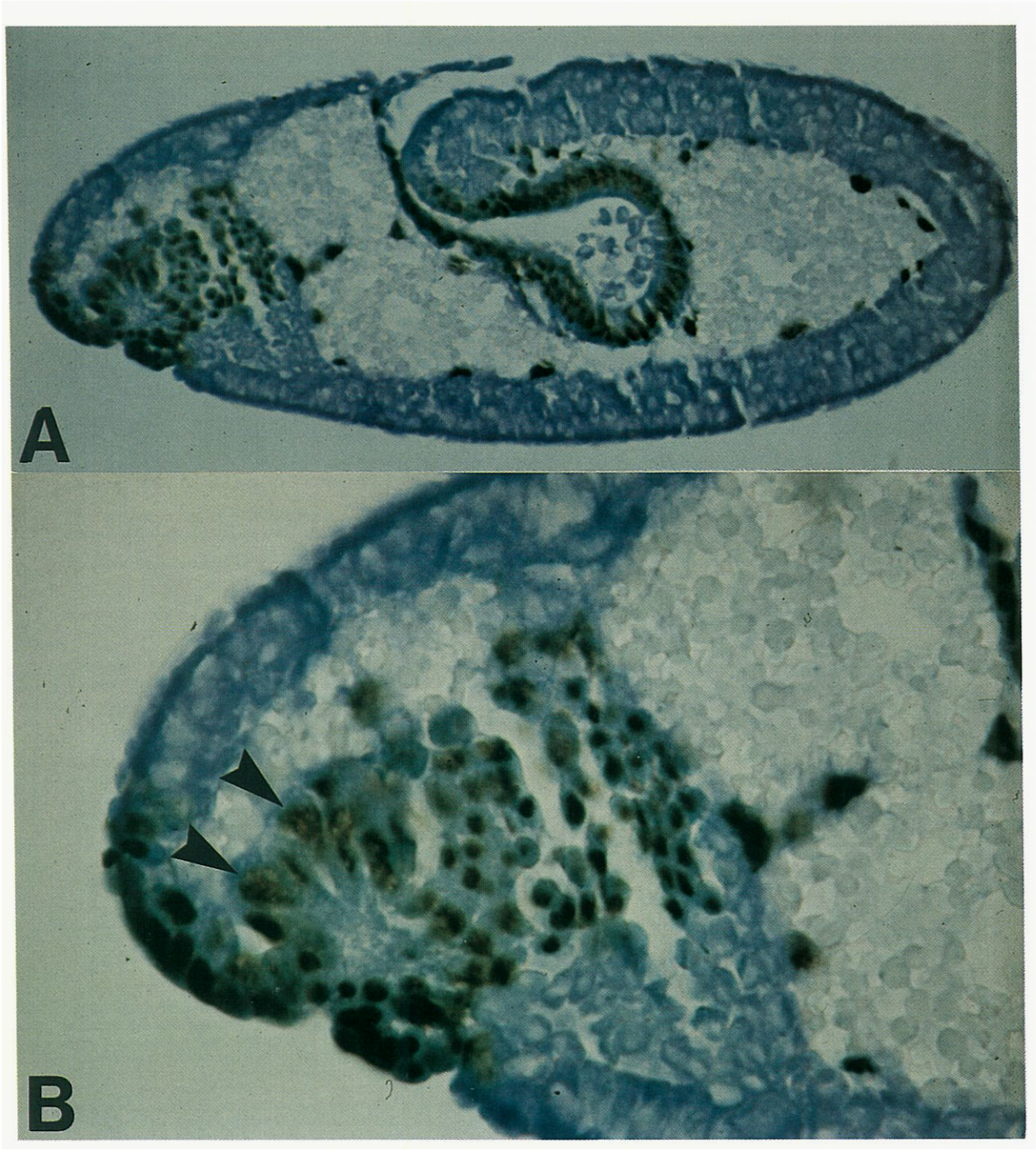

Figure 7. Subcellular Localization of *fkh* Protein

Whole mount preparations of embryos were sectioned after staining with anti-*fkh* antibodies.
(A) Total view of an embryo at germ band elongation.
(B) Enlarged view of the anterior end of the embryo shown in (A). The staining is restricted to the nuclei (arrowheads).

To determine the spatial expression pattern of the *fkh* transcript, we hybridized a radioactively labelled RNA probe to tissue sections of wild-type embryos (Figure 8). Specific hybridization in two terminal domains is detectable shortly before cellularization of the blastoderm. The anterior domain extends from about 95% to 100% egg length (EL; 0% is the posterior, 100% the anterior end [Campos-Ortega and Hartenstein, 1985]), the posterior domain extends from about 0% to 15% EL (Figures 8a and 8b). The two domains appear as slightly dorsally displaced caps covering both poles of the embryo. These two domains correspond reasonably well in both position and extent to the anlagen of ectodermal stomodaeum at the anterior pole and of ectodermal proctodaeum and en-

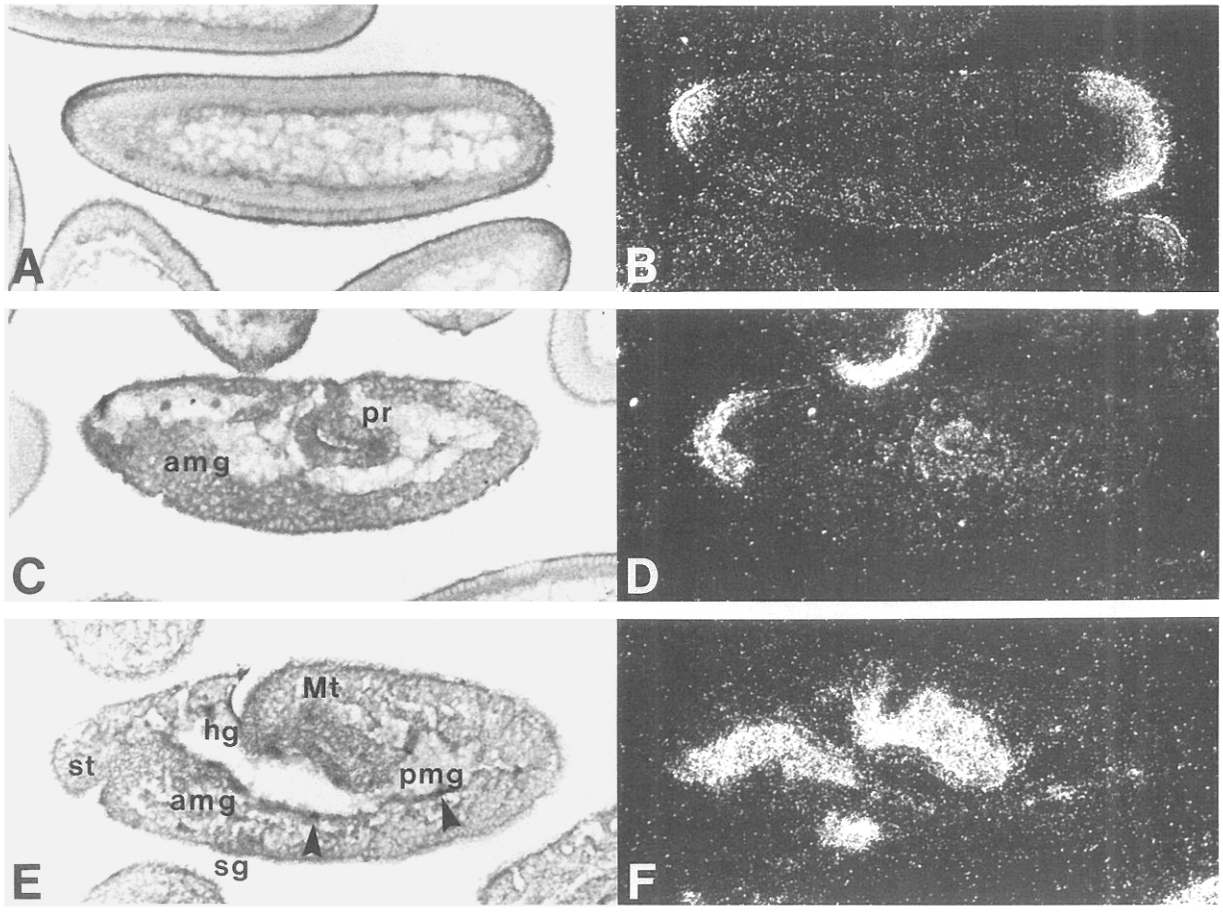

Figure 8. Spatial Expression of *fkh* RNA during Embryonic Development

Tissue sections of paraffin-embedded wild-type embryos were hybridized in situ with a single-stranded RNA probe (see Experimental Procedures). The left panels show bright-field, the right panels corresponding dark-field images of the same, sagittal or parasagittal, sections. Stages are according to Campos-Ortega and Hartenstein (1985). Anterior is to the left, dorsal up.

(A, B) At the end of syncytial and in cellular blastoderm (stage 5), *fkh* transcripts are detected in an anterior and a posterior terminal domain.

(C, D) The posterior domain marks the amnioproctodaeal invagination (pr) in stage 8. In the anterior domain, transcripts start to spread into the primordium of the anterior midgut (amg).

(E, F) At stage 11, the anterior domain includes the invaginated stomodaeum (st) and the anterior midgut primordium (amg). In the posterior domain, hindgut primordium (hg), posterior midgut primordium (pmg), and the outbudding Malpighian tubules (Mt), which are also affected in *fkh* mutant embryos (Jürgens and Weigel, 1988), can be distinguished. Additional sites of *fkh* transcription are the salivary gland placodes (sg) and the periphery of the yolk sac (arrowheads).

dodermal posterior midgut at the posterior pole, as inferred from fate-mapping studies (Hartenstein et al., 1985; Jürgens et al., 1986; Jürgens, 1987). Stomodaeum and proctodaeum give rise to the structures that are homeotically transformed in *fkh* mutant embryos.

The spatial distribution of *fkh* protein in wild-type embryos was visualized by staining whole mount preparations with anti-*fkh* antibodies (Figure 9). *fkh* protein is first detected in the posterior domain at the end of syncytial blastoderm, while the anterior domain is detected only after the beginning of cellularization (Figures 9a, 9b, 9c, and 9d). At the end of cellular blastoderm, the posterior domain has expanded to its final size and exhibits a sharp border at its anterior margin. The posterior domain covers a cap of 0%–13% EL at this stage; the anterior domain covers a cap of 94%–100% EL (Figure 9e). These measurements agree well with the extent of the terminal domains determined by in situ hybridization. The temporal difference between the development of the anterior and posterior domain was noted only at the protein level. However, this temporal difference is quite subtle, and interpretation of in situ hybridization to tissue sections is generally more difficult than interpretation of antibody staining of whole mount preparations, especially when investigating the poles. In contrast to all homeotic selector genes with the exception of *Dfd* (Scott and Carroll, 1987; Chadwick and McGinnis, 1987; Martinez-Arias et al., 1987; Jack et al., 1988), the *fkh* protein can already be detected shortly after the onset of *fkh* transcription. The almost immediate translation of the *fkh* transcript probably reflects the small size of the intronless *fkh* transcription unit compared with the partly giant transcription units in the ANT-C and BX-C (Gehring and Hiromi, 1986).

At the posterior pole, *fkh* gene activity is required in ec-

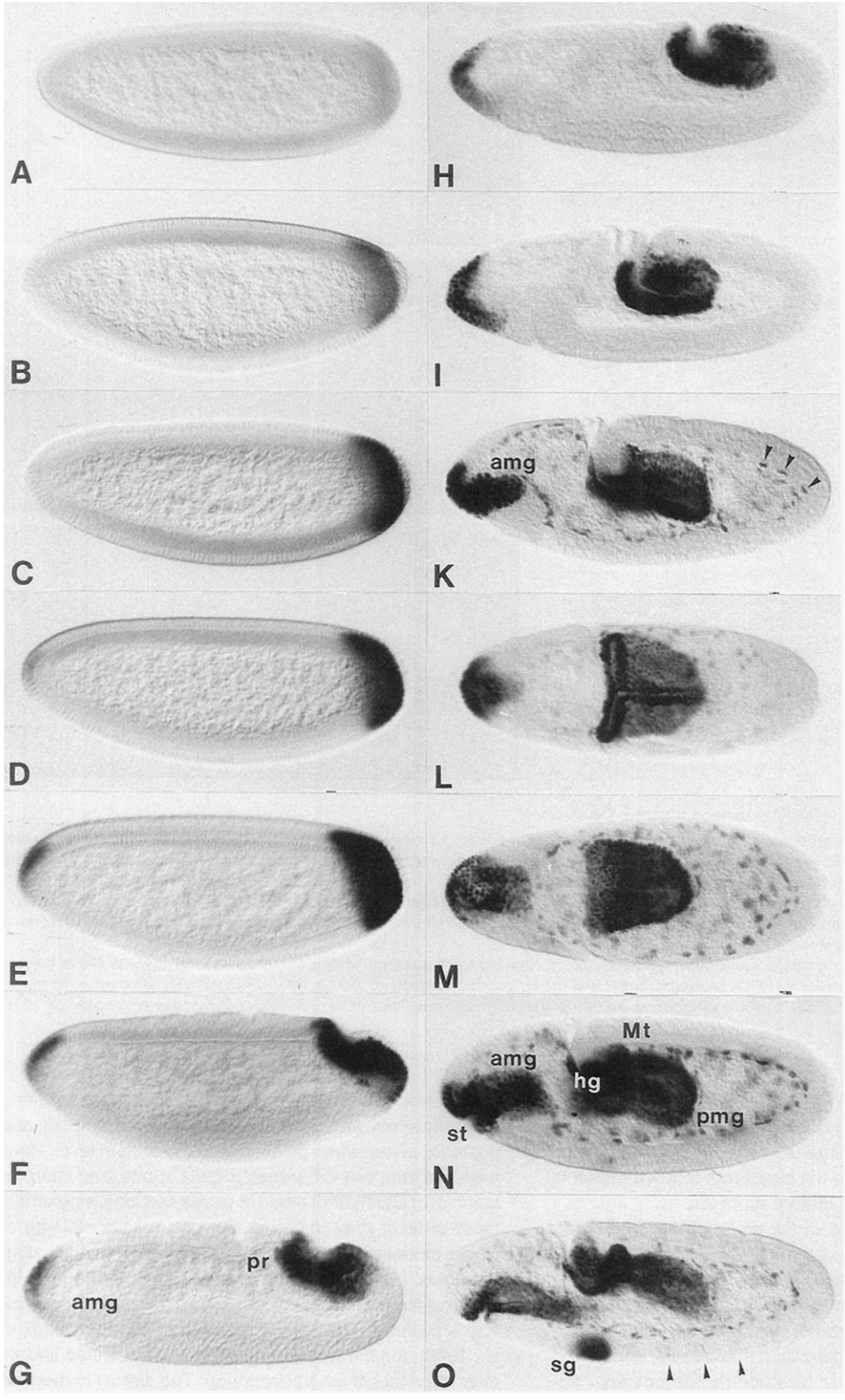

Figure 9. Expression of *fkh* Protein during Embryonic Development

Whole mount preparations of wild-type embryos were stained with anti-*fkh* antibodies (see Experimental Procedures). Except for (L) and (M), optical sections through the sagittal plane with Nomarski optics are shown. Stages are described according to Campos-Ortega and Hartenstein (1985). (A) Stage 4, end of syncytial blastoderm. The posterior domain spreads from the posterior pole.

todermal anlagen posterior to PS 15 (Jürgens and Weigel, 1988). To analyze the distribution of *fkh* protein with respect to parasegmental boundaries, embryos were double-stained with antibodies directed against *fkh* and *fushi tarazu (ftz)* protein. *ftz* belongs to the pair rule class of segmentation genes and is expressed in seven stripes in the early embryo (Hafen et al., 1984; Carroll and Scott, 1985; Krause et al., 1988). Double staining reveals that the posterior *fkh* domain in the early embryo abuts the seventh *ftz* stripe (Figure 10). The anterior margin of each *ftz* stripe marks the anterior border of even-numbered parasegments from PS 2 to PS 14 (Lawrence et al., 1987). With the exception of the seventh *ftz* stripe, each stripe is one parasegment wide. At the onset of gastrulation, the seventh stripe is almost twice as wide as the other stripes; furthermore, *ftz* mutations eliminate pattern elements of both PS 14 and PS 15 (Jürgens, 1987). Thus, the seventh *ftz* stripe obviously spans two parasegments, and its posterior margin demarcates the posterior border of PS 15. Hence, expression of *fkh* protein in the early embryo covers the region behind PS 15. The posterior domain of expression corresponds accurately to the domain of action of the *fkh* gene as determined by phenotypic analysis of *fkh* mutant embryos.

Expression of the *fkh* Gene after the Blastoderm Stage

The posterior domain does not appear to enlarge after the blastoderm stage and follows the amnioproctodaeal invagination during gastrulation and the initial phase of germ-band elongation (Figures 9f and 9g). At the anterior pole, *fkh* expression starts to spread into the invaginating primordium of the anterior midgut, which was initially devoid of *fkh* gene expression (Figures 8c, 8d, 9h, and 9i). By the end of the fast phase of germ-band elongation, the anterior domain has also reached its final size and now includes the ectodermal stomodaeum primordium and the endodermal anterior midgut primordium (Figure 9k). At the same time, expression in the yolk nuclei, which have migrated to the periphery of the yolk sac, becomes apparent. When the germ band is fully extended, the stomodaeum invaginates at the anterior pole, and both initially terminal domains come to lie completely inside the embryo (Figures 9n and 9o). Meanwhile, the salivary gland placodes in the anlage of the labial segment and cells in the primordium of the central nervous system (CNS) have started to express the *fkh* protein (Figures 8e, 8f, 9o).

The expression pattern changes only marginally during later stages of embryogenesis. With the exception of the midgut, *fkh* expression persists until very late stages of embryonic development in all tissues in which it was initially switched on (data not shown).

Aside from the early terminal domains in the ectoderm, *fkh* is expressed in four additional tissues: the developing midgut, salivary glands, nervous system, and the yolk nuclei. Histological analysis of *fkh* mutant embryos had revealed that development of midgut and salivary glands are disturbed in *fkh* mutant embryos (Jürgens and Weigel, 1988). Consistent with the mutant phenotype, *fkh* protein is expressed in their primordia. A mutant phenotype has not been found for the yolk nuclei and the cells in the nervous system, partly due to the lack of suitable cell markers.

Discussion

In this report, we show that the homeotic *fkh* gene of Drosophila is expressed outside parasegments (PS) 0–15, where the ANT-C and BX-C selector genes and the region-specific *sal* gene act. The early expression and the nuclear localization of its gene product make *fkh* similar to the canonical selector genes of ANT-C and BX-C. Its unique protein sequence, however, distinguishes *fkh* from all other homeotic genes and suggests a different evolutionary origin of the *fkh* gene.

The *fkh* Gene Is Expressed Early in the Terminal Regions of the Ectoderm

In *fkh* mutant embryos, the derivatives of stomodaeum and proctodaeum, i.e. foregut and hindgut, are homeotically transformed. Fate-mapping studies have placed the anlagen of stomodaeum and proctodaeum at the anterior

(B–D) Stage 5, cellularization of blastoderm. The posterior domain expands further, and the anterior domain appears. Note the unstained pole cells, which are the germ-line precursors, at the posterior pole.

(E–G) Transition from stage 6 to 7, gastrulation. The posterior domain shifts with the formation of the dorsal plate that carries the pole cells. Shortly thereafter, the dorsal plate begins to sink inwards and will eventually form the amnioproctodaeal invagination (pr). At the anterior end of the ventral furrow, through which the mesoderm invaginates, the anterior midgut primordium (amg), which is not stained by anti-*fkh* antibodies at this stage, becomes visible.

(H, I) Stage 8, germ-band extension. The posterior domain invaginates further and moves cephalad. The anterior domain enlarges and starts to spread interiorly into the anterior midgut primordium.

(K–M) Stage 9. The whole anterior midgut primordium now expresses *fkh*, the anteriorly adjacent stomodaeum anlage, still at the surface, has already shifted ventrally. *fkh*-positive nuclei in the yolk sac correspond to the yolk nuclei that have migrated to the periphery (arrowheads).

(L) Dorsal view.

(M) Ventral view.

(N) Stage 10, fully extended germ band. The stomodaeum (st) invaginates at a position slightly anterior to the anterior midgut invagination. At the border of hindgut (hg) and posterior midgut (pmg) primordia a furrow is formed from which later the Malpighian tubules (Mt) will develop.

(O) Stage 11. The rest of the anterior domain invaginates, and the primordia of anterior and posterior midgut grow caudad. At the posterior margin of the hindgut, the Malpighian tubules bud out. The salivary gland placodes (sg) appear ventrally in the labial segment. *fkh*-positive cells become detectable in the primordium of the CNS (arrowheads).

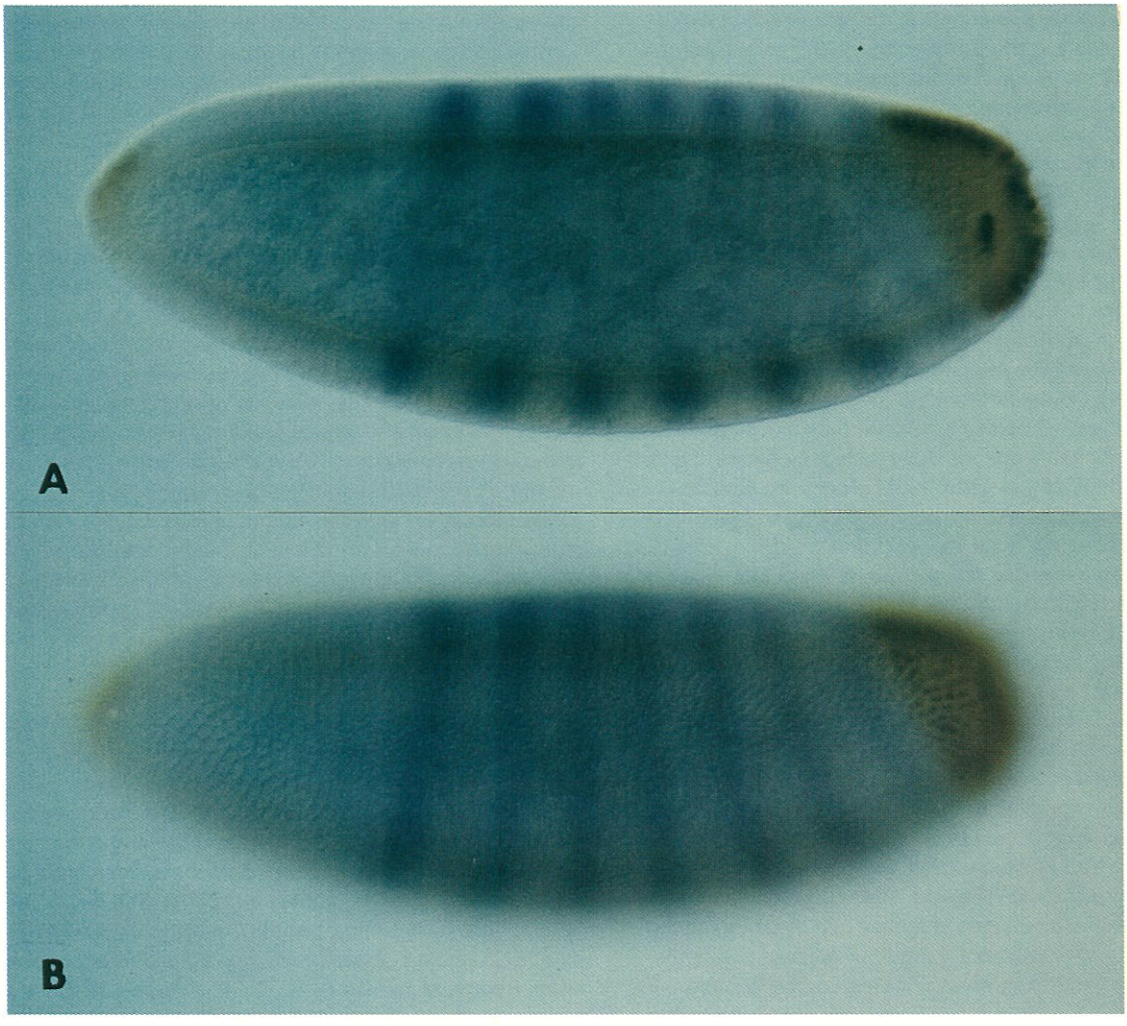

Figure 10. Parasegmental Expression of *fkh*

Whole mount preparations of wild-type embryos were successively stained with anti-*fkh* and anti-*ftz* antibodies (see Experimental Procedures). *ftz* staining is blue; *fkh* staining is brown.

(A) Optical sagittal section of an embryo at the end of cellular blastoderm, shortly before the onset of gastrulation.

(B) Optical tangential section of the same embryo (Nomarski optics). The seventh *ftz* stripe is five nuclei wide at this stage (Carroll and Scott, 1985). The anterior margin of the posterior *fkh* domain is five nuclei behind the anterior margin of the seventh *ftz* stripe, i.e. the posterior *fkh* domain is directly adjacent to the seventh *ftz* stripe. Since *ftz* staining is comparatively weak in this preparation, a zone of lower staining intensity appears anterior of the posterior *fkh* domain. This is due to the fact that *ftz* expression fades away towards the posterior margins of the stripes (Lawrence et al., 1987).

and posterior end of the ectoderm anlage in the early embryo (Hartenstein et al., 1985; Jürgens et al., 1986; Jürgens, 1987). Since the ectodermal anlagen are segmentally determined during blastoderm stage (Akam, 1987; Technau, 1987), any gene participating in this process must be expressed at or before this time. Consistent with playing a role in terminal versus segmental determination, *fkh* gene expression becomes detectable in two terminal domains during blastoderm stage. This also confirms that the phenotypic consequences of the lack of *fkh* gene function are due to a specific requirement of *fkh* gene activity in the anlagen of stomodaeum and proctodaeum.

Based on genetic evidence, we have argued previously that the *fkh* terminal domains correspond to metameric units of the body plan in the Drosophila embryo (Jürgens and Weigel, 1988). This assumption is further corroborated by the parasegmental mode of *fkh* gene expression as determined by comparison with the expression pattern of the pair rule gene *ftz*. The posterior *fkh* domain lies posteriorly adjacent to PS 15. With regard to its parasegment-specific expression, the *fkh* gene behaves similarly to the homeotic selector genes of ANT-C and BX-C. In the early embryo, the members of the ANT-C and BX-C are expressed in register with parasegmental borders (see Akam, 1987; Ingham, 1988). The posterior *fkh* domain respects a parasegmental border in the same way. Unfor-

tunately, because no parasegment-specific landmarks are available for the anterior head, we cannot determine whether this is true of the anterior domain.

In contrast to the homeotic selector genes, *fkh* gene expression in the ectoderm does not become sequentially restricted to its terminal domains, but rather is activated from early on only in its appropriate limits. The extensive modulation of spatial expression of homeotic selector genes appears to reflect the complex regulatory interactions involving different classes of segmentation genes, other selector genes, and *trans*-regulatory genes such as the *Pc* group genes (see Ingham, 1988). The comparatively simple expression pattern of *fkh* confirms our conclusions about its region-specific action derived from phenotypic analysis of mutant embryos (Jürgens and Weigel, 1988).

Differential Regulation of the Anterior and Posterior *fkh* Domain

The *fkh* protein appears later in the anterior than in the posterior domain. In addition, the adjacent anlagen of the anterior and posterior midgut, respectively, are included in these domains at different stages of development. We therefore think it likely that *fkh* expression is under distinct regulatory control in the two domains. Potential regulators of early *fkh* gene expression are the maternal and zygotic segmentation genes of the terminal class, i.e. the maternal genes of the *torso* group and the zygotic gap gene *tailless (tll)* (Nüsslein-Volhard et al., 1987; Klingler, et al., 1988; Strecker et al., 1988), and the anterior pattern organizer *bicoid (bcd)* (Frohnhöfer and Nüsslein-Volhard, 1986). Amorphic mutations in the maternal terminal genes delete all structures of the posterior *fkh* domain, whereas mutations in the zygotic terminal gene *tll* affect only the ectodermal part of the posterior *fkh* domain. Therefore, the control of the posterior *fkh* domain probably involves hitherto unidentified zygotic factors. None of the terminal gene mutations completely deletes the structures derived from the anlagen included in the anterior *fkh* domain. These structures are dependent on *bcd* gene activity, which might play a crucial role in regulating the *fkh* anterior domain. The situation is, however, further complicated by the fact that in *bcd* mutant embryos, posterior *fkh* dependent structures develop at the anterior end.

Differences between the anterior and posterior *fkh* domain are also apparent in embryos carrying a weak *fkh* allele or the recombinant P-element P[NS-*fkh*] in an amorphic background. In both cases, posterior structures develop almost normally, whereas the anterior domain displays severe defects (see Figure 3). Specifically, in embryos carrying P[NS-*fkh*], no *fkh* protein can be detected in the ectodermal part of the anterior domain, whereas all other domains express *fkh* protein, although at lower levels than in wild type. In contrast, *fkh* protein is initially present in the anterior domain of embryos carrying the weak fkh^{XT8} allele, but disappears later in development (D. Weigel, unpublished data). This places important *cis*-regulatory sequences downstream of the *fkh* transcription unit, since the hypomorphic alleles delete only sequences downstream of the transcribed region. The most distant breakpoint is about 30 kb remote from the 3′ end of the *fkh* transcription unit, suggesting an unusually large 3′ regulatory region on which the products of upstream genes could act.

The *fkh* Gene Is Expressed in a Variety of Tissues in the Late Embryo

Already at the blastoderm stage, the posterior *fkh* domain is not restricted to the anlage of ectodermal proctodaeum, but also includes the anlage of endodermal posterior midgut. The anterior midgut, initially devoid of *fkh* gene expression, becomes *fkh*-positive during germ-band extension. Although *fkh* mutant embryos do develop a midgut, it does not differentiate properly (Jürgens and Weigel, 1988). Simultaneous expression of *fkh* in both the ectodermal and the endodermal parts of the gut is intriguing, but so far we have no evidence for a role of *fkh* in early steps of midgut development. More information could be obtained from studying genes that are expressed early in the midgut primordia of wild-type embryos. Expression of *fkh* in anterior and posterior midgut primordia correlates with the finding that the cells of both primordia have equivalent developmental potency (Technau and Campos-Ortega, 1986). The salivary glands are missing in *fkh* mutant embryos (Jürgens and Weigel, 1988), and in agreement with this observation, *fkh* is expressed in the developing salivary glands. Whether *fkh* gene expression in the developing nervous system is essential is still unknown.

Expression of *fkh* in a variety of different tissues apart from its primary domains, the ectodermal portions of the gut, suggests redeployment of the *fkh* gene during subsequent developmental decisions that need not be of a homeotic nature. Experimental evidence for multiple functions in very different aspects of development has been obtained for a number of genes, including segmentation genes of the gap and pair rule classes and the *daughterless* gene, which is required for sex determination as well as for formation of the nervous system (Gloor, 1954; Gaul, 1988; Doe et al., 1988a, 1988b; Caudy et al., 1988).

The *fkh* gene Encodes a Nuclear Protein of Novel Structure

The *fkh* gene promotes terminal as opposed to segmental development. In the absence of *fkh* gene product, this developmental switch does not occur. Since decisions between different developmental pathways entail differential gene activity, switch genes are likely to affect transcriptional regulation of subordinate genes. Many of the genes involved in the Drosophila segmentation gene hierarchy encode nuclear proteins that are characterized by one of two conserved motifs—a homeodomain or zinc fingers (see Ingham, 1988). Both motifs are not confined to Drosophila segmentation genes, but represent more widely occurring protein structures mediating transcriptional regulation via binding to specific DNA sequences.

The sequence of the *fkh* protein does not contain any similarity to other known proteins, and thus does not pro-

vide us with any hint at the mode of action of the *fkh* gene. However, the nuclear localization of its protein product suggests that *fkh* also exerts its function via transcriptional regulation of other genes. To substantiate this presumption, we must identify genes that are under the control of the *fkh* gene product.

Evolutionary Considerations

The fact that the region-specific homeotic genes *sal* and *fkh* are not as closely related to one another as are the homeotic selector genes can be surprising only at first sight. A more detailed consideration of the processes in which both genes are involved suggests that, relative to *sal*, the *fkh* function is evolutionarily much older. Insects, the predominant class of modern arthropods, evolved from annelid-like ancestors that possessed a segmented body plan. Their body plan, though, did not exhibit any significant regional specialization apart from the nonsegmental endpieces of acron and telson and the openings of foregut and hindgut at the anterior and posterior pole (Anderson, 1973). In a very similar way to the arthropods, foregut and hindgut develop in annelids from the primordia of stomodaeum and proctodaeum, the primary domains of *fkh* gene action in Drosophila (Dawydoff, 1959; Anderson, 1973). We infer from this that *fkh* gene activity may have been required already in the annelid-like ancestors of modern arthropods.

The specialization and subsequent integration of the anterior-most trunk segments into a primitive head was probably the first step in the evolution of arthropods from their annelid-like ancestors (Anderson, 1973; Lauterbach, 1973). Since *sal* gene activity is required to distinguish head from trunk parasegments, *sal* might be regarded as a genetic counterpart of this evolutionary achievement (Jürgens, 1988). Thus, the requirement of *sal* gene activity appeared much later than the requirement of *fkh* gene activity.

Experimental Procedures

Unless otherwise noted, standard methods were employed according to Hames and Rickwood (1981), Maniatis et al. (1982), Roberts (1986), and Carroll and Laughon (1988).

Chromsomal Walking

A chromosomal walk (Bender et al., 1983) was carried out with different phage and cosmid libraries. Walking was greatly facilitated by alternate use of phages and cosmids, since whole phages could be used to screen cosmid libraries and vice versa.

Isolation of cDNAs

Various cDNA libraries, kindly provided by L. Kauvar (Poole et al., 1985), were screened with different genomic probes encompassing almost the complete walk. cDNAs for the three proximal-most transcripts were isolated by using whole cosmid DNA as a probe. Twenty-one *fkh* cDNA clones were isolated out of approximately 600,000 phages in the E7 library. Extensive restriction mapping confirmed their sequence similarity to the sequenced *fkh* cDNAs. All cDNAs were either truncated at one of the three internal EcoRI sites or not of full length.

Germ-Line Transformation

The 15.3 kb NotI–SpeI fragment was subcloned from a genomic cosmid into NotI–XbaI-digested pW8 vector (Klemenz et al., 1987). About 600 embryos of the *w sn*^{w} stock were injected with the recombinant plasmid pWNS (300 μg/μl) and the helper plasmid pπ25.7wc (100 μg/μl) according to Spradling (1986). Three out of two hundred thirty-three G0 flies produced transformed progeny from which the lines *P[NS-*fkh*1, 2, 3]* were established. Transformed flies were crossed to *fkh*^{3}*/TM3* heterozygous flies and the nonbalancer progeny backcrossed inter se. In each case, embryos with a novel cuticle phenotype that was identical for all three lines were produced from these crosses. The recombinant P elements were genetically mapped to the second or fourth chromosome (*P[NS-*fkh*1, 3]*) and to the third chromosome (*P[NS-*fkh*2]*).

DNA Sequencing of Wild-Type and Mutant Alleles

Sequencing by the dideoxynucleotide method (Sanger et al., 1977) was carried out using M13 vectors (Yanisch-Perron et al., 1985). Besides the universal M13 primer, various internal primers derived from already determined sequences were used. Sequence of the wild-type genomic DNA was determined either on random fragments generated by sonification (Deininger, 1983) or on subcloned restriction fragments. With the exception of approximately 500 bp adjacent to the flanking BglII site, sequence was determined on both strands. Sequence of cDNAs was determined on subcloned restriction fragments. The predicted protein sequence was compared with the SwissProt data base using the programs MicroGenie (Beckman) and PC/Gene (Genofit) on an IBM PC/AT.

To clone mutant DNA from four *fkh* alleles, a SalI restriction fragment length polymorphism was exploited. In the mutant *fkh* alleles, the region corresponding to the wild-type *fkh* open reading frame is contained within a 7.2 kb SalI fragment that carries an additional SalI site in the balancer chromosome *TM3, Sb Ser.* Genomic DNA of flies heterozygous for each *fkh* mutant chromosome and the balancer chromosome was SalI-digested, and a size-selected partial library was constructed in the insertion vector λZAP (Stratagene) digested with XhoI. Positive clones were identified with appropriate probes and in vivo subcloned according to the manufacturer's instructions. BamHI–XhoI fragments (see Figure 5) were sequenced from the BamHI site at position +556 bp of the wild-type open reading frame. For all alleles, two independently isolated clones were sequenced. With the exception of *fkh*^{1}, the mutant sequence was confirmed on the other strand.

In Situ Hybridization to Tissue Sections

In situ hybridization to tissue sections was peformed as described by Ingham et al. (1985) with minor modifications. As template for synthesizing ^{35}S-UTP-labeled RNA probes, a genomic 1.5 kb DraI–NsiI fragment subcloned into pBluescript (Stratagene; subclone p15DN) was used.

Antibody Preparation

A genomic 1.4 kb BamHI–PstI fragment coding for the C-terminal 332 amino acids of the predicted *fkh* protein was subcloned into pBluescript, isolated as a BamHI–HindIII fragment, and subcloned into the pUR288 vector (Rüther and Müller-Hill, 1983). After transformation of the recombinant pURBH plasmid into XL1 bacteria (Stratagene), a *lacZ–fkh* fusion protein of about 160 kd apparent molecular weight (154 kd predicted molecular weight) was produced upon induction by IPTG. The fusion protein was purified according to Rio et al. (1986) with minor modifications. In contrast to their protocol, after dialysis of the urea extract, the precipitated material was recovered and solubilized in 50 mM HEPES (pH 6.9), 0.1% SDS. The solution was dialyzed against 50 mM HEPES (pH 6.9) and subsequently stored at −80°C. The fusion protein, which was approximately 70% pure as determined on a Coomassie-stained polyacrylamide gel, was used for immunization and for affinity purification. A young female rabbit was immunized with several hundred μg of fusion protein resolved on a polyacrylamide gel according to standard procedures and boosted twice after 4 and 8 weeks. After the second boost, high titer of antibodies directed against the *lacZ–fkh* fusion protein as determined by Western blot analysis were present in the serum of the rabbit. To prepare an affinity column, the enriched fusion protein was coupled to Affigel (BioRad) in 50 mM HEPES (pH 6.9) according to the manufacturer's instructions. After washing the column with PBS, 0.5% Triton X-100 and PBS and under elution conditions (see below) and final equilibration with PBS, 0.1% Tween20, 0.1 M NaCl, serum was mixed 1:1 with PBS, adjusted to 0.1% Tween20, 0.1 M NaCl, and loaded onto the column. After extensive washing with PBS, 0.1% Tween20, 0.9 M NaCl, the antigen was eluted

with 4 M $MgCl_2$. Protein-containing fractions were pooled, dialyzed against PBS, and anti-β-galactosidase antibodies removed by passing the antibody solution twice over a β-galactosidase column. Purity of the concentrated antibody preparation was checked by Western blot analysis using different bacterial extracts (data not shown). *fkh*^{3} embryos were known from DNA sequence analysis to produce only a truncated form of the protein lacking almost 90% of the wild-type sequence against which the antibodies are directed at the C-terminus (see Results). When embryos derived from *fkh*^{3} heterozygous parents were stained with the affinity-purified antibody preparation, one-quarter of these embryos showed only unspecific background (data not shown). Therefore, our antibody preparation must be specific for the Drosophila *fkh* protein.

Antibody Staining of Embryos

Whole mount preparations of embryos were stained using the VECTASTAIN ABC-peroxidase system (Vector Laboratories) with DAB as substrate according to Macdonald and Struhl (1986) with minor modifications. For the double labeling experiment with anti-*fkh* and anti-*ftz* antibodies, both produced in rabbits, the different sensitivities of the normal ABC kit and the ABC Elite kit were exploited. The embryos were first incubated with anti-*fkh* antibodies at a low concentration and then reacted with the ABC Elite-peroxidase. After washing, the stained embryos were incubated with anti-*ftz* antibodies at twice the normal concentration and subsequently reacted with the normal ABC-glucose oxidase using NBT as substrate. Since the first antibodies were used at too low a concentration to be effectively detected by the normal ABC, the second reaction is specific for the antibodies of the second incubation. For tissue sections, stained embryos were embedded into Paraplast (Monoject Scientific) and processed following the method for in situ hybridization.

Acknowledgments

We thank our colleagues in Tübingen and Munich for helpful discussion, Drs. S. Cohen, U. Gaul, M. Klingler, M. Pankratz, and V. Siegel for critical reading of the manuscript, Drs. J. A. Campos-Ortega and U. Dietrich for the E7Δ6 cDNA clone, Dr. D. Tautz for synthesizing oligonucleotides, Dr. H. Krause for anti-*ftz* antibodies, and R. Groemke-Lutz for photographic prints. D. W. was a fellow of the Boehringer Ingelheim Fonds. This work was supported by the Deutsche Forschungsgemeinschaft (Leibniz-Programm and DFG grant Ja312/5-1).

The costs of publication of this article were defrayed in part by the payment of page charges. This article must therefore be hereby marked "*advertisement*" in accordance with 18 U.S.C. Section 1734 solely to indicate this fact.

Received December 22, 1988; revised February 22, 1989.

References

Akam, M. (1987). The molecular basis for metameric pattern in the *Drosophila* embryo. Development *101*, 1–22.

Anderson, D. T. (1973). Embryology and Phylogeny in Annelids and Arthropods. (Oxford: Pergamon Press).

Baker, N. E. (1988). Localization of transcripts from the *wingless* gene in whole *Drosophila* embryos. Development *103*, 289–298.

Baumgartner, S., Bopp, D., Burri, M., and Noll, M. (1987). Structure of two genes at the *gooseberry* locus related to the *paired* gene and their spatial expression during *Drosophila* embryogenesis. Genes Dev. *1*, 1247–1267.

Bender, W., Spierer, P., and Hogness, D. S. (1983). Chromosomal walking and jumping to isolate DNA from the *Ace* and *rosy* loci and the *bithorax* complex in *Drosophila melanogaster*. J. Mol. Biol. *168*, 17–33.

Campos-Ortega, J. A., and Hartenstein, V. (1985). The embryonic development of *Drosophila melanogaster*. (Berlin: Springer-Verlag).

Carroll, S. B., and Scott, M. P. (1986). Zygotically active genes that affect the spatial expression of the *fushi tarazu* segmentationgene during early *Drosophila* embryogenesis. Cell *45*, 113–122.

Carroll, S. B., and Laughon, A. (1988). Production and purification of polyclonal antibodies to the foreign segment of β-galactosidase fusion proteins. In DNA Cloning: A Practical Approach, Volume III, D. M. Glover, ed. (Oxford: IRL Press), pp. 89–111.

Caudy, M., Grell, E. H., Dambly-Chaudière, C., Ghysen, A., Jan, L. Y., and Jan, Y. N. (1988). The maternal sex determination gene *daughterless* has zygotic activity necessary for the formation of peripheral neurons in *Drosophila*. Genes Dev. *2*, 843–852.

Cavener, D. R. (1987). Comparison of the consensus sequence flanking translation start sites in *Drosophila* and vertebrates. Nucl. Acids Res. *15*, 1353–1361.

Chadwick, R., and McGinnis, W. (1987). Temporal and spatial distribution of transcripts from the *Deformed* gene of *Drosophila*. EMBO J. *6*, 779–789.

Dawydoff, C. (1959). Ontogenèse des annélides. In Traité de Zoologie, Volume V, P.-P. Grassé, ed. (Paris: Masson), pp. 594–686.

Deininger, P. (1983). Random subcloning of sonicated DNA: application to shotgun DNA sequence analysis. Anal. Biochem. *129*, 216–223.

Desplan, C., Theis, J., and O'Farrell, P. H. (1985). The *Drosophila* developmental gene *engrailed* encodes a sequence specific DNA binding activity. Nature *318*, 630–635.

Desplan, C., Theis, J., and O'Farrell, P. H. (1988). The sequence specificity of homeodomain–DNA interaction. Cell *54*, 1081–1090.

Doe, C. Q., Hiromi, Y., Gehring, W. J., and Goodman, C. S. (1988a). Expression and function of the segmentation gene *fushi tarazu* during *Drosophila* neurogenesis. Science *239*, 170–175.

Doe, C. Q., Smouse, D., and Goodman, C. S. (1988b). Control of neuronal fate by the *Drosophila* segmentation gene *even-skipped*. Nature *333*, 376–378.

Frei, E., Schuh, R., Baumgartner, S., Burri, M., Noll, M., Jürgens, G., Seifert, E., Nauber, U., and Jäckle, H. (1988). Molecular characterization of *spalt*, a homeotic gene required for head and tail development in the *Drosophila* embryo. EMBO J. *7*, 197–204.

Frohnhöfer, H. G., and Nüsslein-Volhard, C. (1986). Organization of anterior pattern in the *Drosophila* embryo by the maternal gene *bicoid*. Nature *324*, 120–125.

Gaul, U. (1988). Ph.D. thesis, University Tübingen, Tübingen, Federal Republic of Germany.

Gehring, W. J., and Hiromi, Y. (1986). Homeotic genes and the homeobox. Annu. Rev. Genet. *20*, 147–173.

Gloor, H. (1954). Phänotypen der Heterozygoten bei der unvollständig dominanten, homozygot letalen Mutante *Kr* (=*Krüppel*) von *Drosophila melanogaster*. Arch. Jul. Klaus. Stiftung *29*, 277–287.

Hafen, E., Kuroiwa, A., and Gehring, W. J. (1984). Spatial distribution of transcripts from the segmentation gene *fushi tarazu* during Drosophila embryonic development. Cell *37*, 833–841.

Hames, B. D., and Rickwood, D., eds. (1981). Gel electrophoresis of proteins: a practical approach. (Oxford: IRL Press).

Hartenstein, V., Technau, G. M., and Campos-Ortega, J. A. (1985). Fate-mapping in wild-type *Drosophila melanogaster*. Roux's Arch. Dev. Biol. *194*, 181–195.

Hoey, T., and Levine, M. (1988). Divergent homeo box proteins recognize similar DNA sequences in *Drosophila*. Nature *332*, 858–861.

Ingham, P. W. (1988). The molecular genetics of embryonic pattern formation in *Drosophila*. Nature *335*, 25–34.

Ingham, P. W., Howard, K. R., and Ish-Horowicz, D. (1985). Transcription pattern of the *Drosophila* segmentation gene *hairy*. Nature *318*, 439–445.

Jack, T., Regulski, M., and McGinnis, W. (1988). Pair-rule segmentation genes regulate the expression of the homeotic selector gene, *Deformed*. Genes Dev. *2*, 635–651.

Jürgens, G. (1987). Segmental organization of the tail region in the embryo of *Drosophila melanogaster*. A blastoderm fate map of the cuticle structures of the larval tail region. Roux's Arch. Dev. Biol. *196*, 141–157.

Jürgens, G. (1988). Head and tail development of the *Drosophila* embryo involves *spalt*, a novel homeotic gene. EMBO J. *7*, 189–196.

Jürgens, G., and Weigel, D. (1988). Terminal versus segmental development in the *Drosophila* embryo: the role of the homeotic gene *fork head*. Roux's Arch. Dev. Biol. *197*, 345–354.

Jürgens, G., Lehmann, R., Schardin, M., and Nüsslein-Volhard, C. (1986). Segmental organization of the head in the embryo of *Drosophila melanogaster*. A blastoderm fate map of the cuticle structures of the larval head. Roux's Arch. Dev. Biol. *195*, 359–377.

Klemenz, R., Weber, U., and Gehring, W. J. (1987). The *white* gene as a marker in a new P-element vector for gene transfer in *Drosophila*. Nucl. Acids Res. *15*, 3947–3959.

Klingler, M., Erdélyi, M., Szabad, J., and Nüsslein-Volhard, C. (1988). Function of *torso* in determining the terminal anlagen of the *Drosophila* embryo. Nature *335*, 275–277.

Knust, E., Dietrich, U., Tepass, U., Bremer, K. A., Weigel, D., Vässin, H., and Campos-Ortega, J. A. (1987). EGF homologous sequences encoded in the genome of *Drosophila melanogaster*, and their relation to neurogenic genes. EMBO J. *6*, 761–766.

Krause, H. M., Klemenz, R., and Gehring, W. J. (1988). Expression, modification, and localization of the *fushi tarazu* protein in *Drosophila* embryos. Genes Dev. *2*, 1021–1036.

Lauterbach, K.-E. (1973). Schlüsselereignisse in der Evolution der Stammgruppe der Euarthropoda. Zool. Beitr. (N.F.) *19*, 251–299.

Lawrence, P. A., Johnston, P., Macdonald, P. M., and Struhl, G. (1987). Borders of parasegments in *Drosophila* embryos are delimited by the *fushi tarazu* and *even-skipped* genes. Nature *328*, 440–442.

Macdonald, P. M., and Struhl, G. (1986). A molecular gradient in early *Drosophila* embryos and its role in specifying the body pattern. Nature *324*, 537–545.

Maniatis, T., Fritsch, E. F., and Sambrook, J. (1982). Molecular Cloning: A Laboratory Manual (Cold Spring Harbor, New York: Cold Spring Harbor Laboratory).

Martinez-Arias, A., and Lawrence., P. A. (1985). Parasegments and compartments in the *Drosophila* embryo. Nature *313*, 639–642.

Martinez-Arias, A., Ingham, P. W., Scott, M., and Akam, M. E. (1987). The spatial and temporal deployment of *Dfd* and *Scr* transcripts during development of *Drosophila*. Development *100*, 673–680.

Nüsslein-Volhard, C., Frohnhöfer, H. G., and Lehmann, R. (1987). Determination of anteroposterior polarity in *Drosophila*. Science *238*, 1675–1681.

Poole, S. J., Kauvar, L. M., Drees, B., and Kornberg, T. (1985). The *engrailed* locus of Drosophila: structural analysis of an embryonic transcript. Cell *40*, 37–43.

Rio, D. C., Laski, F. A., and Rubin, G. M. (1986). Identification and immunochemical analysis of biologically active Drosophila P element transposase. Cell *44*, 21–32.

Roberts, D. B., ed. (1986). *Drosophila*: A Practical Approach. (Oxford: IRL press).

Rüther, U., and Müller-Hill, B. (1983). Easy identification of cDNA clones. EMBO J. *2*, 1791–1794.

Sanger, F., Nicklen, S., and Coulson, A. R. (1977). DNA sequencing with chain-terminating inhibitors. Proc. Natl. Acad. Sci. USA *74*, 5463–5467.

Scott, M. P., and Carroll, S. B. (1987). The segmentation and homeotic gene network in early *Drosophila* development. Cell *51*, 689–698.

Spradling, A. C. (1986). P element-mediated transformation. In *Drosophila*: A Practical Approach, D. B. Roberts, ed. (Oxford: IRL Press), pp. 175–197.

Strecker, T. R., Merriam, J. R., and Lengyel, J. A. (1988). Graded requirement for the zygotic terminal gene, *tailless*, in the brain and tail region of the *Drosophila* embryo. Development *102*, 721–734.

Tautz, D., Trick, M., and Dover, G. A. (1986). Cryptic simplicity in DNA is a major source of genetic variation. Nature *322*, 652–654.

Technau, G. M. (1987). A single cell approach to problems of cell lineage and commitment during embryogenesis of *Drosophila melanogaster*. Development *100*, 1–12.

Technau, G. M., and Campos-Ortega, J. A. (1986). Lineage analysis of transplanted individual cells in embryos of *Drosophila melanogaster*. III. Commitment and proliferative capabilities of pole cells and midgut progenitors. Roux's Arch. Dev. Biol. *195*, 489–498.

Yanisch-Perron, C., Vieria, J., and Messing, J. (1985). Improved M13 phage cloning vectors and host strains: nucleotide sequences of M13mp18 and pUC19 vectors. Gene *33*, 103–119.

Notes Added in Proof

The temporal difference between the anterior and posterior *fkh* domain has been meanwhile confirmed on the RNA level by whole-mount in situ hybridization.

The *fkh* sequence has been submitted to GenBank under accession number J03177.